

# RSC Advances



This article can be cited before page numbers have been issued, to do this please use: N. Allam, W. Sharmoukh, W. M. I. Hassan and P. C. GROS, *RSC Adv.*, 2016, DOI: 10.1039/C6RA16458G.



This is an *Accepted Manuscript*, which has been through the Royal Society of Chemistry peer review process and has been accepted for publication.

*Accepted Manuscripts* are published online shortly after acceptance, before technical editing, formatting and proof reading. Using this free service, authors can make their results available to the community, in citable form, before we publish the edited article. This *Accepted Manuscript* will be replaced by the edited, formatted and paginated article as soon as this is available.

You can find more information about *Accepted Manuscripts* in the [Information for Authors](#).

Please note that technical editing may introduce minor changes to the text and/or graphics, which may alter content. The journal's standard [Terms & Conditions](#) and the [Ethical guidelines](#) still apply. In no event shall the Royal Society of Chemistry be held responsible for any errors or omissions in this *Accepted Manuscript* or any consequences arising from the use of any information it contains.

# Design and Synthesis of New Ru-Complexes as Potential Photo-sensitizers: Experimental and TD-DFT insights

Walid Sharmoukh<sup>1</sup>, Walid M.I. Hassan<sup>2</sup>, Philippe C. Gros<sup>3</sup> and Nageh K. Allam<sup>4,\*</sup>

<sup>1</sup>*Department of Inorganic Chemistry, National Research Centre, Dokki, Giza 12622, Egypt*

<sup>2</sup>*Department of Chemistry, Faculty of Science, Cairo University, Giza 12613, Egypt*

<sup>3</sup>*Photosens, Université de Lorraine, UMR SRSMC, Vandoeuvre-Lès-Nancy, Nancy, France*

<sup>4</sup>*Energy Materials Laboratory (EML), School of Sciences and Engineering, The American University in Cairo, New Cairo 11835, Egypt. \*E-mail: [nageh.allam@aucegypt.edu](mailto:nageh.allam@aucegypt.edu).*

## Abstract

We report density functional theory (DFT) and time-dependent density functional theory (TDDFT) calculations on a novel organic ligand and a novel class of ruthenium complexes; cis-RuL<sub>2</sub>X<sub>2</sub> with L = 2, 2'-bipyridine-6, 6'-bis ethyl ester phosphonate and phosphonic acid, X = Cl, CN or NCS. The calculations show that cis-configurations are more stable than the trans-counterparts. The DFT results have been used to help designing such novel complexes for potential use as a sensitizer. We demonstrate the opportunity to synthesize such complexes with high purity. The synthesis of these complexes relies on the preparation of the key intermediates cis-Ru(2,2'-bipyridine-6,6'-bisdiethyl ester phosphonate)Cl<sub>2</sub>. These complexes were characterized by <sup>1</sup>H, <sup>13</sup>C, and <sup>31</sup>P NMR, elemental analysis and FTIR spectroscopy. The NCS complex shows the smallest optical band gap followed by the Cl and CN complexes, respectively, with the highest performance upon use as a sensitizer in dye-sensitized solar cells.

**Keywords:** DFT; optical properties; dipole moment; Ru complexes; NMR spectroscopy.

## 1        1. Introduction

2  
3        With the looming energy crisis and the depletion of petroleum and natural-gas reserves,  
4 various ways have been investigated to convert the sun light directly into chemical fuel or  
5 electricity.<sup>1</sup> However, the capital cost of such devices is still inconvenient for large-scale  
6 implementation. To this end, dye-sensitized solar cells (DSSCs) have attracted considerable  
7 attention due to their high quantum efficiency giving the opportunity of low-cost conversion of  
8 solar energy into electrical power.<sup>2</sup> The ongoing research in DSSCs is mainly focusing on the  
9 optimization of all cell components; namely, the photoactive material, the dye and the redox  
10 electrolyte.<sup>3</sup>

11        The development of optically active sensitizers over a wide region of the solar spectrum  
12 is a hot topic nowadays. In particular, ruthenium (Ru)-based complexes have been extensively  
13 used as sensitizers.<sup>4,5</sup> Ruthenium metal has been particularly investigated for a number of  
14 reasons:<sup>6</sup> (1) it has octahedral geometry that enable the introduction of specific ligands in a  
15 controlled manner; (2) it forms very inert bonds with imine nitrogen centers; (3) it possesses  
16 various stable and accessible oxidation states. However, the main problem limiting the further  
17 development of sensitizers is the fact that dyes with high absorption coefficients has narrow  
18 bands and vice-versa. Consequently, the optimization of sensitizers is mainly based on “*guess-*  
19 *and-check*” procedures. A more systematic approach is required in order to find optimum  
20 sensitizers with the required specifications. In this regard, density function theory (DFT)  
21 calculations are considered ideal to solve the “*guess-and-check*” problem involved in the design  
22 of DSSCs as well as solar hydrogen production systems. Specifically, it can be used to study the  
23 changes in the optical and electronic structures of the sensitizers.

24        Herein, we report detailed DFT calculations on new cis- ruthenium complexes with  
25 coordinated bipyridine bisphosphonate ligands. Our DFT findings were confirmed via the

1 preparation and characterization of such sensitizers and their use in dye-sensitized solar cell  
2 devices.

3

## 4 **2. Computational and Experimental Methods and Materials**

5

### 6 **2.1 Density Functional Theory and Time-dependent Density Functional Theory**

7

8 The molecular geometry for all complexes and ligands was fully optimized using 6-31+G  
9 mixed basis sets for C, H, N, O, P, Cl and S atoms and effective core potential  
10 LANL2/LANL2DZ basis set<sup>7-10</sup> for Ru atom with the density functional (DFT) level. The DFT  
11 calculations were carried out using the hybrid three-parameter density functional method  
12 abbreviated as B3LYP, which includes Beck's 3-parameter gradient exchange correction  
13 function (B3)<sup>11</sup> and the Lee, Yang and Parr correlation functional<sup>12,13</sup>. The B3LYP method  
14 typically provides energetic better than Hartree–Fock method<sup>14</sup> and can reproduce better  
15 geometrical parameters comparable to the experimental values than any other method<sup>15</sup>. No  
16 symmetry constrains were implemented during all the geometry optimization procedures. All  
17 possible configurations for the complexes were calculated and the one shown here is the lowest  
18 in energy or the global minimum for each complex. All the geometry optimization, vibrational  
19 frequency calculations were done using the Gaussian 09 software package<sup>16</sup>. The optimized  
20 structures were visualized using Chemcraft version 1.6 packages<sup>17</sup>. The bond dissociation  
21 energy of A-B bond is calculated by subtracting the total energy of the optimized geometry for  
22 AB molecule from single point energy of its constituents A and B at the same geometry, which is  
23 more accurate than substrating it from optimized energy of isolated molecules as this would  
24 include some part of possible conformation relaxation energy changes. Ionization potential and  
25 electron affinity of cation and anion total energy subtracted from neutral total energy at  
26 optimized geometry without further optimization as electron movements are assumed to be faster

1 than nuclear ones. Time-dependent DFT calculations were done on optimized geometry using  
2 number of excited states equal to 10. Exciton binding energies were estimated by the difference  
3 between LUMO and HOMO in DFT and in TD-DFT calculation. The electronic absorption  
4 spectra were created using convolution with Gaussian function using Gauss View Software<sup>18</sup>  
5 using UV-Vis peak Half-Width at half height of 0.1 eV.

## 6 **2.2 Experimental Materials and Synthesis**

7  
8 All start materials are high grade chemicals and solvents that were purchased from Sigma  
9 Aldrich. The solvents were distilled before use. <sup>1</sup>H, <sup>13</sup>C NMR and <sup>31</sup>P NMR spectra were  
10 recorded using 5 mm tube on a Bruker AC-250 (250.133 and 62.896 MHz, respectively) or  
11 Varian Gemini 2000 (199.976 and 50.289 MHz, respectively) and were referenced to  
12 tetramethylsilane (TMS) and triphenylphosphine.

### 13 • **Synthesis and Characterization of 2,2'-bipyridine N,N'-Dioxide**

14  
15 2, 2'-bipyridine (4g, 25.61 mmol) was dissolved in 50 ml chloroform. mCPBA m-  
16 chloroperbenzoic acid (22.1 g, 64.03 mmol) dissolved in 200 ml chloroform was added slowly (4  
17 h) to this solution at zero temperature. After the completion of addition, the solution was stirred  
18 for another 2 days. The reaction was filtered off and quenched by the addition of methanol for  
19 one day. The precipitation filtered and dried at room temperature; (Yield 92 %)

20 <sup>1</sup>H NMR (200 MHz, D<sub>2</sub>O, ppm): 8.31- 8.27(d, 2H), 7.67-7.54(m, 6 H);

21 <sup>13</sup>C NMR (100 MHz, D<sub>2</sub>O, ppm) 139.69, 137.60, 129.23, 126.75, 126.31

22

### 23 • **Synthesis and Characterization of 6,6'-dicyano 2,2'-bipyridine**

24 2,2'-bipyridine N,N'-Dioxide (6 g, 31.88 mmol) and potassium cyanide (12.3 g, 189 mmol)  
25 were dissolved in 100 ml water. Methylene chloride 40 ml and benzoyl chloride (15.69g, 111.6  
26 mmol) were added slowly upon three hours at zero temperature. After completion of addition,  
27 the mixture was stirred at 0 °C for about four hours. The solution was filtered and quenched by  
28 ethanol for one day. The precipitation filtered and dried at room temperature to Yield 75%.

1  $^1\text{H}$  NMR (200 MHz,  $\text{CDCl}_3$ , ppm): 8.74-8.69(dd, 2H), 8.06- 7.98(t, 2H), 7.79 – 7.75(dd, 2H);  
2  $^{13}\text{C}$ NMR (100 MHz,  $\text{CDCl}_3$ , ppm) 153.83, 138.78, 131.48, 129.01, 123.88, 116.24; EA found: C,  
3 69.95; H, 2.83; N, 27.39%. Theoretical: 69.90; H, 2.93; N, 27.17%).

4  
5 • **Synthesis and Characterization of 6,6'-bis(ethoxycarbonyl) 2,2'-bipyridine**

6 6,6'- dicyano 2,2'- bipyridine (5g, 24.25 mmol) was dissolved in 80 ml ethanol and 34 ml  
7 of sulfuric acid was added slowly to solution. The reaction mixture was heated to reflux for one  
8 day. The solution poured over 100 g of ice and stirred for 2 h, then extracted with methylene  
9 chloride. The solution was washed with brine three times. After that the solution dried over  
10 magnesium sulfate anhydrous and reduced to yellow white solid (85%).

11  $^1\text{H}$  NMR (200 MHz,  $\text{CDCl}_3$ , ppm) 8.79 – 8.74(dd, 2H), 8.16- 8.12(dd, 2H), 8.02- 7.94)(t, 2H),  
12 4.55 – 4.44(q, 4H), 1.50- 1.43(t, 6H);  
13  $^{13}\text{C}$ NMR (100 MHz,  $\text{CDCl}_3$ , ppm) 163.31, 153.63, 146.01, 136.18, 123.57, 122.84, 60.04 ppm.  
14 EA found, C, 64.22; H, 5.37; N, 9.54%. Theoretical; C, 63.99; H, 5.37; N, 9.33%)

15  
16 • **Synthesis and Characterization of 6,6'-Bis (hydroxymethyl)-2, 2'-bipyridine**

17 6,6'-Di-functionalized bipyridine was prepared from 6,6'-dibromo-2,2'-bipyridine via lithium-  
18 bromide exchange, followed by addition of suitable electrophiles such as N,N-dimethyl formamide, to  
19 give dialdehyde <sup>(19)</sup>. The 6, 6'-bis (hydroxymethyl)-2, 2'-bipyridine was prepared following the  
20 procedure reported in literature <sup>(20)</sup>.

21  $^1\text{H}$  NMR (400 MHz,  $\text{CDCl}_3$ ): 8,63-8,31(d,2H), 7,86-7.79(t,2H), 7,27-7.24(d, 2H), 4.83(s, 4H),  
22 3.98(bs,2H) ppm;  
23  $^{13}\text{C}$ NMR (100 MHz,  $\text{CDCl}_3$ ): 160.14, 150.23, 138.69, 120.90, 119.04, 62.33 ppm;  
24 Anal, Calcd for  $\text{C}_{12}\text{H}_{10}\text{N}_2\text{O}_2$ , C, 66.65; H, 5.59; N, 12.96. Found; C, 66.46; H, 5.69; N, 13.18.

25  
26 • **Synthesis and Characterization of 6,6'-Bis(bromomethyl)-2,2'-bipyridine:-**

27 6,6'-bis(hydroxymethyl)-2,2'-bipyridine (6.39 mmol, 1,3g) was dissolved in a mixture of 48%  
28 HBr (30 ml) aqueous solution and concentrated sulfuric acid (10.5 ml). The resulting solution was  
29 refluxed for 8h and then allowed to cool to room temperature. Then, 75 ml of water was added. The  
30 pH was adjusted to neutral with NaOH solution. The resulting precipitate was filtered, and washed  
31 with water. The product was dissolved in chloroform (60 ml) and filtered. The solution was dried over

1 anhydrous magnesium sulfate and evaporated under vacuum to dryness. Product was isolated as a  
2 white powder; (Yield 88%)

3  $^1\text{H}$  NMR (400 MHz,  $\text{CDCl}_3$ ):  $\delta$  4.60(4H, s,  $\text{CH}_2$ ); 7.38(2H, d,  $J=5\text{Hz}$ , aryl H on C5 and C5); 8.45(2H,  
4 s, aryl H on C3 and C3); 8.68 (2H, d,  $J=5\text{Hz}$ , aryl H on C6 and C6) ppm.

5  $^{13}\text{C}$  NMR (100 MHz,  $\text{CDCl}_3$ ):  $\delta$  165.20, 155.45, 137.91, 123.55, 120.50, 34.1 ppm.

6 Anal, Calcd for  $\text{C}_{12}\text{H}_{10}\text{N}_2\text{Br}_2$  :- C, 42.1; N, 8.18; H, 2.92. Found: C, 42.36; N, 7.86; H, 2.82.

7

8 • **Synthesis and Characterization of 6,6'-Bis(diethylmethy phosphonate)-2,2'-**  
9 **bipyridine**

10 A chloroform (15 ml) solution of 6, 6'-Bis (bromomethyl)-2, 2'-bipyridine (0.3g, 8.77mmol) and  
11 2.91g (17.7 mmol) of triethyl phosphate was refluxed for 5 h under nitrogen. The excess phosphate  
12 was removed under high vacuum, and then the crude product was obtained as yellow-white powder;  
13 Yield 85%

14  $^1\text{H}$  NMR (400 MHz,  $\text{CDCl}_3$ ):  $\delta$  1.30 (12H), 3.5(4H,  $\text{CH}_2\text{P}$ ), 4.10(8H,  $\text{OCH}_2$ ), 7.35-7.38(2H), 8.34-  
15 8.37(2H), 8.62(2H) ppm.

16  $^{13}\text{C}$  NMR (100 MHz,  $\text{CDCl}_3$ ):  $\delta$  155.58, 152.08 (d,  $J=7.9\text{ Hz}$ ), 137.27(d,  $J=2.2\text{ Hz}$ ), 124.16(d,  $J=4.6$   
17 Hz), 119.03(d,  $J=3\text{ Hz}$ ), 62.15(d,  $J=6.8\text{ Hz}$ ), 37.33, 35.99 and 16.31(d,  $J=6\text{Hz}$ ) ppm.

18 Elemental anal, Calcd for,  $\text{C}_{20}\text{H}_{30}\text{N}_2\text{O}_6\text{P}_2$ : C, 52.63; N, 6.14; H, 6.63. Found: C, 52.5; N, 5.93; H, 6.7.

19

20

21 • **Synthesis and Characterization of Ru [(6, 6'-( $\text{CH}_2\text{PO}_3\text{Et}_2$ ) $_2$ bpy)] $_2\text{Cl}_2$ .**

22 A solution of 6,6'-Bis(diethylmethy phosphonate)-2,2'-bipyridine (295 mg, 0.636mmol)  
23 and  $\text{LiCl}$ (286 mg, 6.8 mmol), and  $\text{Ru}(\text{DMSO})_4\text{Cl}_2$  (205 mg, 0.423 mmol) in dry DMF (15 ml)  
24 was refluxed for 7 h under nitrogen in the dark at (160- 170  $^\circ\text{C}$ ). After the solution was cooled  
25 to room temperature, methylene chloride was added and the precipitate was filtered and washed  
26 with methylene chloride. Finally the precipitate was washed with diethyl Esther (three times 10  
27 ml). After the compound was dried in a vacuum, and then the crude product was obtained as  
28 brown-white (yield 85 %). the complex was used as such in the next step.

29  $^1\text{H}$  NMR (400 MHz,  $\text{D}_2\text{O}$ ):  $\delta$  1.20(t,  $J=6.8\text{Hz}$ , 12H,  $\text{CH}_3$ ), 1.22(t,  $J=7.2\text{ Hz}$ , 12H,  $\text{CH}_3$ ), 3.9(m,  $J$   
30 = 7.2 Hz, 8H,  $\text{CH}_2$ ), 3.8(m,  $J=7.2\text{ Hz}$ , 8H,  $\text{CH}_2$ ), 3.4(d,  $J=20.8\text{ Hz}$ , 8H,  $\text{PCH}_2$ ), 7.96(dd,  $J=7.2$

1 Hz, 4H And J=2.4 Hz, 4H, H3,H4), 7.54(dd, J= 1.6 Hz And, J= 5.2 Hz, 2H, Hs) And J= 2, J= 7.2,  
2 2H, H5') ppm.

3 <sup>13</sup>CNMR (100 MHz, D<sub>2</sub>O): δ 155.625, 155.6, 155.4, 155.33, 138.561, 124.727, 124.689, (d, J=  
4 3.8 Hz), 120.573(d, J= 3 Hz), 61.527, 61.467 (d, J= 6 Hz, CH<sub>2</sub>), 37.71, 37.05, 36.458 (t, CH<sub>2</sub>P)  
5 and 16.082, 16.021(d, J= 6.1 Hz) ppm.

6 <sup>31</sup>PNMR (400 MHz, D<sub>2</sub>O): 28.167 ppm

7 Elemental anal: Calcd for (C<sub>40</sub>H<sub>60</sub>Cl<sub>2</sub>N<sub>4</sub>O<sub>12</sub>P<sub>4</sub>Ru), C<sub>32</sub>H<sub>44</sub>Cl<sub>2</sub>N<sub>4</sub>O<sub>12</sub>P<sub>4</sub>Ru), theoretical; C, 39.5, H,  
8 4.56, N, 5.67. Found, C, 41.0, H, 4.77, N, 6.1.

9 <sup>1</sup>H NMR (400 MHz, CD<sub>3</sub>OD): δ 1.15(t, J= 7.2Hz, 12H, CH<sub>3</sub>), 1.13(t, J= 6.8 Hz, 12H, CH<sub>3</sub>),  
10 3.8(d, J=7.2 Hz, 8H, CH<sub>2</sub>), 3.86(m, J=7.2Hz, 8H, CH<sub>2</sub>), 3.3(d, J= 23.2Hz, 8H, PCH<sub>2</sub>), 7.41(dd,  
11 J= 8 Hz, 4H), 7.8(dd, J= 7.6 Hz and J= 8 Hz, 4H), 8.09(dd, J= 8 Hz, 4H) ppm.

12 <sup>13</sup>CNMR (100 MHz, CD<sub>3</sub>OD): δ 158.45, (d, J= 9.1 Hz), 155.49, 139.799, 126.35, (d, J= 6.8 Hz),  
13 119.73, 61.72(d, J=6.1Hz, CH<sub>2</sub>)38.40, 37.12, 17.18, (d, J= 7.6 Hz) ppm.

14  
15 • **Synthesis and Characterization of Ru[(6,6'-(CH<sub>2</sub>PO<sub>3</sub>H<sub>2</sub>)<sub>2</sub>bpy)]<sub>2</sub>Cl<sub>2</sub>.**

16 A solution of Ru [(6, 6'-(CH<sub>2</sub>PO<sub>3</sub>Et<sub>2</sub>)<sub>2</sub>bpy)]<sub>2</sub>Cl<sub>2</sub> (2.18 g, 0.212 mmol) in 15 ml of 18%  
17 HCl was refluxed for 15 h. after that, the solvent was evaporated on a rotary evaporator. The  
18 resulting yellow-brown was dissolved in a minimal amount of water and evaporated. Then dry in  
19 high vacuum to obtain a title compound in 90 % yield.

20 <sup>1</sup>H NMR (400 MHz, D<sub>2</sub>O): δ 2.71(P-OH, 8H), 3.59( d, J= 20.8 Hz, CH<sub>2</sub>-P, 8H), 7.80(dd, J= 68  
21 Hz, 4H), 8.311( dd, J= 68 Hz, 8H), notice: when we were using D<sub>2</sub>O as a solvent , we found two  
22 peaks was overlap in one peak (H3,H4), and for methanol we found three peaks for pyridine ring.

23 <sup>1</sup>H NMR (400 MHz, CD<sub>3</sub>OD): δ 8.39(dd, J=7.6 Hz, 4H), 8.27(4H) and 7.78(dd, J=8 Hz, 4H),  
24 3.64, (d, J= 21.6 Hz, CH<sub>2</sub>-P, 8H) and 2.63( P-OH, 8H) ppm.

25 <sup>13</sup>CNMR (100 MHz, D<sub>2</sub>O): δ 153.04, 146.718, 143.686, 128.176, 122.028, 36.292 and 35.041  
26 ppm.

27 <sup>31</sup>PNMR (400 MHz, D<sub>2</sub>O): Two peaks, at 7.76 ppm and 25.718 ppm (reference PPh<sub>3</sub>).

28 Elemental anal, Calcd. For (C<sub>24</sub>H<sub>28</sub>Cl<sub>2</sub>N<sub>4</sub>O<sub>12</sub>P<sub>4</sub>Ru.H<sub>2</sub>O), theoretical C, 33.82, H, 3.44, N, 6.38.  
29 Found, C, 32.54, H, 3.29, N, 6.15.

30

31

1 • **Synthesis and Characterization of Ru[(6,6'-(CH<sub>2</sub>PO<sub>3</sub>H<sub>2</sub>)<sub>2</sub>bpy)]<sub>2</sub>(CN)<sub>2</sub>.**

2 A solution of Ru [(6, 6'-(CH<sub>2</sub>PO<sub>3</sub>H<sub>2</sub>)<sub>2</sub>bpy)]<sub>2</sub>Cl<sub>2</sub>, (50mg, 0.058 mmol) and KCN (75.5mg, 1.0  
3 mmol) were dissolved in a mixture of water 10 ml and methanol 10 ml in a round- bottomed  
4 flask 150 ml. And then the solution was purged with nitrogen. The flask was then covered with  
5 aluminum foil and heated at reflux for 15h in dark. After the solution cooled at room temperature,  
6 a grade acetone was added to the crude reaction mixture and the precipitate was filtered off and  
7 washed with acetone. The result of complexes is to yield 80% brown white. To purify this  
8 complex, dissolve in a minimum amount of water and purified by column chromatography using  
9 silica-gel (LH20) as stationary phase and water as eluent.

10 <sup>1</sup>H NMR (400 MHz, CD<sub>3</sub>OD): δ 2.15(P-OH, 8H), 3.14(d, J= 19.6Hz, CH<sub>2</sub>-P, 8H), 7.31(dd, J=  
11 7.6 Hz, 4H), 7.81(dd, J= 7.6 Hz and J= 8 Hz, 4H), 7.88(dd, J= 8 Hz, 4H) ppm.

12 <sup>13</sup>CNMR (100 MHz, CD<sub>3</sub>OD) δ 171.19 (CN), 158.6(d, J= 6.9Hz), 154.86, 138.19, 124.49(d,  
13 J=3.8), 119.55, 40.51, 39.33 ppm.

14 <sup>31</sup>PNMR (400 MHz, CD<sub>3</sub>OD), one peak at 25.23 ppm ref.pph<sub>3</sub>.

15 IR (KBr) (CN) at 2052Cm<sup>-1</sup>.

16  
17 • **Synthesis and Characterization of [Ru[(6,6'-(CH<sub>2</sub>PO<sub>3</sub>H<sub>2</sub>)<sub>2</sub>bpy)]<sub>2</sub>(NCS)<sub>2</sub>.**

18 A solution of Ru [(6, 6'-(CH<sub>2</sub>PO<sub>3</sub>H<sub>2</sub>)<sub>2</sub>bpy)]<sub>2</sub>Cl<sub>2</sub>, (50mg, 0.058 mmol) and KSCN  
19 (22.25mg , 2.32 mmol), were dissolved in a mixture of water 10 ml and methanol 10 ml in a  
20 round- bottomed flask 150 ml, And then the solution was purged with nitrogen. The flask was  
21 then covered with aluminum foil and heated at reflux for 15h in the dark. After the solution  
22 cooled at room temperature, a grade acetone was added to the crude reaction mixture and the  
23 precipitate was filtered off and washed with acetone. The result of complexes is to yield 85%  
24 brown.

25 <sup>1</sup>H NMR (400 MHz, CD<sub>3</sub>OD): δ 8.38(d, J=8Hz, 1H), 8.26(t, J=8Hz, 1H), 7.78(d, J=8Hz, 1H),  
26 3.57(d, J=20.8Hz, 2H) ppm.

27 <sup>1</sup>H NMR (400 MHz, D<sub>2</sub>O): δ 8.15(broad peak, 2H), 7.67(broad peak, 1H), 3.49(d, J=42Hz, 2H)  
28 ppm.

29 <sup>13</sup>CNMR (400 MHz, D<sub>2</sub>O): δ 154.0, 153.9, 146.95, 146.93, 143.3, 127.92, 127.87, 121.57, 36.79  
30 and 35.58 ppm

31 <sup>31</sup>PNMR (400 MHz, CD<sub>3</sub>OD): one peak at 25.093 ppm ref.pph<sub>3</sub>

32 IR (KBr) (NCS) at 2113 cm<sup>-1</sup>.

1       • **Fabrication and Testing of the DSSCs.**

2           The DSSC devices were fabricated and tested as detailed in our previous work<sup>21</sup>.

4       **3. Results and Discussion**

6           The optimized geometry of the cis- and trans-configurations of the synthesized sensitizers  
7 is shown in Figures 1 and 2, respectively with their energetic parameters are summarized in  
8 Table 1. Our calculations showed that cis-configurations are more stable than the trans-  
9 counterparts. The P=O bond length was calculated to be 1.49 Å in all complexes. The Ru-N bond  
10 (connected to the organic part) length was found to be similar in all complexes with a range from  
11 2.15 Å to 2.20 Å. Furthermore, the difference between the cis- and trans- configurations is less  
12 than 1%, indicating that the main change in bond lengths is around the Cl, CN and NCS ligands.  
13 In the cis-configurations, the Cl-Ru-Cl, NC-Ru-CN and SCN-Ru-NCS bond angles are 86.9°,  
14 93.7° and 91.1°, respectively. On the other hand, in the trans-configurations, the Cl-Ru-Cl, NC-  
15 Ru-CN and SCN-Ru-NCS bond angles are 176.4°, 179.5° and 179.3°, respectively. In NCS  
16 complexes, the N-C-S bond angle is 177.8° and 179.5° for the cis- and trans-configurations,  
17 respectively. In case of the CN complexes, only hydrogen bonds are formed between the N of the  
18 CN group and H of phosphate group. Note that this interaction does not exist in the other two  
19 complexes. The calculations showed that two hydrogen bonds with average length of 1.77 Å are  
20 observed in the trans-configuration while only one hydrogen bond with 1.73 Å is formed in case  
21 of the cis-configuration due to geometrical orientation of the phosphate groups.

22           The Ru-Cl, Ru-CN and Ru-NCS bond lengths are 2.18 Å, 1.98 Å and 2.11 Å and 2.49 Å,  
23 2.05 Å and 2.06 Å for cis- and trans-configurations, respectively. It is worth mentioning that the  
24 longer bond lengths in case of Ru-Cl may be the reason for the greater total energy difference  
25  $\Delta E_T$  between cis- and trans-configuration of this complex relative to the others. The energy of

1 the highest occupied molecular orbital ( $E_{\text{HOMO}}$ ) and the lowest unoccupied molecular orbital  
2 ( $E_{\text{LUMO}}$ ) for the complexes under study are summarized in Table 1. The energy gap ( $\Delta E$ ) between  
3  $E_{\text{LUMO}}$  and  $E_{\text{HOMO}}$  is inversely proportional to the reactivity of the complex. The reactivity as  
4 function of  $\Delta E$  is in the order  $\text{Cl} > \text{NSC} > \text{CN}$  and  $\text{NSC} > \text{Cl} > \text{CN}$  for trans- and cis-  
5 configurations, respectively. The dipole moment of the cis-configuration is larger than that of the  
6 trans-counterpart. The bond dissociation energy between Ru metal and ligand has been  
7 calculated. The Ru-Cl, Ru-NCS and Ru-CN bond energies are 75.70, 96.19 and 118.89, and  
8 97.63, 115.19 and 151.99 kcal/mol for trans- and cis-configurations, respectively. These numbers  
9 clearly show that the strength of the inorganic ligands is in the order  $\text{CN} > \text{NCS} > \text{Cl}$ . It further  
10 explains the greater stability of cis- over trans-configuration by at least 20%. On the other hand,  
11 the average Ru-N bond (where N is in the organic ligand) dissociation energies do not show that  
12 greater variance where they are 27.11, 32.89 and 35.09, and 34.13, 35.97 and 35.78 kcal/mol for  
13 Cl, NSC and CN complexes with trans- and cis-configurations, respectively. The NBO charges  
14 on Ru are 0.13, -.017 and -0.32 for NCS, Cl and CN complexes, respectively. The most positive  
15 charge is observed on P atom, which is almost 2.4 in all complexes. However, the most negative  
16 charge is observed on adjacent O atom in the P=O with a value of about -1.1 in all complexes.

17 The optical parameters have been theoretically studied for the cis-conformer only and the  
18 main characteristics are summarized in Table 2. The calculation of ionization potential (IP) and  
19 electron affinity (EA) was done by subtracting the total energy of the ionic complex from neutral  
20 one at the same geometry. It is worth mentioning that the IP and EA seem to be shifted by about  
21 1 eV relative to the  $E_{\text{HOMO}}$  and  $E_{\text{LUMO}}$ . In addition, time-dependent density functional theory  
22 (TD-DFT) calculations were performed to estimate the optical electronic absorption spectra and  
23 exciton binding energies, with the detailed data represented in Table 3. The NCS complex shows

1 the smallest optical band gap, the highest oscillator strength and the lowest exciton binding  
2 energy followed by the Cl and CN complexes, respectively, indicating a better performance for  
3 use as a sensitizer in solar cells application. The electronic absorption spectra are shown for the  
4 three complexes in Figure 3. The CN and NCS have three bands at 385 nm, 455nm and 505nm,  
5 and 461nm, 610nm and 671nm, respectively. On the other hand, the Cl complex spectra have  
6 almost one main band at about 530 nm and other bands seem to be overlapped underneath and  
7 appearing as shoulders. As a general trend, the HOMO and HOMO-1 orbitals are either  $\pi$  orbital  
8 on CN and NCS or p-orbital on the Cl along with d-orbital from Ru atom, see Figure 4. The  
9 LUMO and LUMO+1 are  $\pi^*$  orbital localized on one of the two bipyridine ring. The LUMO+2  
10 and LUMO+4 are also  $\pi^*$  orbital on both of the two bipyridine ring. Furthermore, all the  
11 calculated electronic absorption spectra involve transitions from d- orbital on metal along with  
12 orbitals on Cl, CN or NCS to orbitals on bipyridine rings.

13 Based on the promising DFT results, herein, we show the possibility to synthesize such  
14 complexes. However, we will limit our discussion to the cis-Ru complexes as an example. The  
15 investigated complexes are of the general formula cis-RuL<sub>2</sub>X<sub>2</sub> with L = 2,2'-bipyridine- 6,6'-  
16 bis(diethyl methyl phosphonate) and 2,2'-bipyridine- 6,6'- bis(methylphosphoric acid). The  
17 preparation of this type of complexes usually involves two steps.<sup>(22,23)</sup> The first complex consists  
18 of refluxing two equivalent of the bidentate ligand L with 1 equivalent of ruthenium trichloride in  
19 DMF to yield a cis—RuL<sub>2</sub>Cl<sub>2</sub>. In the second step, the diethyl phosphate was hydrolysed to  
20 phosphonic acid, and then the chloride ligands are substituted by potassium thiocyanate or  
21 potassium cyanide. This is achieved by heating in a mixture of methanol or ethanol and water to  
22 prepare complex that contains cyanide and thiocyanate. The preparation of complexes with  
23 different positions (such as 4, and 5) has been previously patented by Grätzel et al.<sup>(24)</sup> However,

1 no preparation and characterization of ligand and complexes were reported in the open literature.  
2 Herein, we report on the synthesis of new ligand and new complexes, which are shown in Schemes  
3 1 and 2.

4 Starting from the phosphonated bipyridine as a ligand, these complexes were prepared  
5 using Ru(DMSO)<sub>4</sub>Cl<sub>2</sub> and RuCl<sub>3</sub> in water to get highly pure complexes. This could be clearly seen  
6 from the <sup>1</sup>H NMR spectrum of the crude reaction mixture that indicated a lower amount of  
7 impurities when Ru (DMSO)<sub>4</sub>Cl<sub>2</sub> was used. This is probably due to the use of a ruthenium (II)  
8 precursor with weakly binding ligands (DMSO). A purification step was necessary to remove tris-  
9 bipyridine ruthenium complex that was formed during the reaction. The resulting complexes were  
10 purified and crystallized using column chromatography. The diethyl ester phosphonate groups  
11 were fully hydrolyzed by heating the complexes in hydrochloric acid solution. Chloride ligand  
12 exchange with thiocyanate or cyanide was subsequently performed in water with an excess of  
13 monodentate ligands. These complexes were found to be soluble in methanol and water with a  
14 larger solubility at basic pH.

15 The NMR spectra of the complexes were measured in D<sub>2</sub>O and CD<sub>3</sub>OD solutions to  
16 achieve sufficiently large concentrations, compatible with fast spectrum recording and high  
17 signal-to-noise ratio. The <sup>1</sup>H NMR spectra of all complexes show six sharp and well-resolved  
18 signals in the aromatic region, corresponding to the six magnetically inequivalent protons of the  
19 bipyridine (Figure 5). Using D<sub>2</sub>O as a solvent, the downfield shifted protons resonance peaks can  
20 be assigned to the protons H<sub>3</sub> and H<sub>4</sub> that are merged in one peak. On the other hand, upon using  
21 CD<sub>3</sub>OD as solvent, H<sub>3</sub> and H<sub>4</sub> peaks were found to be very close to each other. The assignment is  
22 based on the assumption that deshielding of the protons can be due to an induced magnetic field  
23 created by the ring current on bipyridine aromatic moieties. This deshielding is only significant

1 at short distance and therefore affects only protons that are close to the bipyridine. In this case,  
2 we found that the complexes are cis-octahedral, with two equivalent bipyridine ligands. In  
3 complex (I) in Scheme 2, the two 6, 6'-methylene phosphonate ethyl ester groups ( $\text{CH}_2\text{PO}_3\text{Et}$ )  
4 are inequivalent and they give rise to four multiplets. Therefore, the observed patterns are in  
5 agreement with the cis geometry of the complexes. The results were also confirmed via  $^{13}\text{C}$  and  
6  $^{31}\text{P}$  NMR spectra, which were recorded in  $\text{D}_2\text{O}$  and  $\text{CD}_3\text{OD}$  as solvents, see the supporting  
7 information. The Trans geometry would have resulted in simpler NMR due to the higher  
8 symmetry and would have yielded only three peaks in the aromatic region due to the four  
9 magnetically equivalent pyridine units.

10 Infrared (IR) spectra were recorded in KBr pellets, and the  $\nu_{\text{CN}}$  bands of complex (III)  
11 and (IV) were located, respectively at  $2052\text{ cm}^{-1}$  and  $2113\text{ cm}^{-1}$ , see the supporting information  
12 for more details. It was demonstrated that the band appears around  $2110\text{ cm}^{-1}$  can be assigned to  
13 N-bound thiocyanate,<sup>(25,26)</sup>. Note that it is shifted to lower energy for the S-bound complex to  
14  $2052\text{ cm}^{-1}$ .

15 To validate the results, dye-sensitized solar cell devices were fabricated using the  
16 synthesized complexes as sensitizers to  $\text{TiO}_2$  nanotubes under AM 1.5 illumination (Figure 6 and  
17 Table 4), as detailed in our previous report. Note that the power conversion efficiency (PCE)  
18 increases in the order  $-\text{SCN} > -\text{CN} > -\text{Cl}$ , resulting in PCE of 1.91, 2.38 and 2.9%, respectively.  
19 Note that those efficiencies are at least twice that reported for the same complexes with the  
20 substituents in the 4- and 5- positions<sup>27</sup>, confirming the importance of the position of the  
21 functional group in determining the performance of the Ru-complexes.

22  
23  
24

## 1 Conclusion

2  
3 DFT and TDDFT calculations were performed on cis-[Ru(bipyridine)<sub>2</sub> (phosphonic  
4 acid)<sub>2</sub>]X<sub>2</sub> where X= Cl, CN complexes. Due to geometrical orientation of the phosphate groups,  
5 two hydrogen bonds with average length of 1.77 Å were observed in the trans-configuration with  
6 only one hydrogen bond with 1.73 Å is formed in case of the cis-configuration. The order of  
7 reactivity as function of ΔE was found to be in the order Cl > NSC > CN and NSC > Cl > CN for  
8 trans- and cis- configurations, respectively. The dipole moment of the cis-configuration is larger  
9 than that of the trans-counterpart. The NCS complex shows the smallest optical band gap, the  
10 highest oscillator strength and the lowest exciton binding energy followed by the Cl and CN  
11 complexes, respectively, indicating a better performance for use as a sensitizer in solar cells  
12 application. The CN and NCS have three bands at 385 nm, 455 nm and 505 nm, and 461 nm, 610  
13 nm and 671 nm, respectively. These complexes were found to be soluble in methanol and water  
14 with a larger solubility at basic pH. The cis-configuration of such novel ruthenium complexes was  
15 prepared and characterized by several spectroscopic methods. Upon their use as photosensitizers in  
16 DSSC devices, the power conversion efficiency (PCE) increases in the order -SCN > -CN > -Cl,  
17 resulting in PCE of 1.91, 2.38 and 2.9%, respectively. We hope that our work will open a new  
18 route toward the synthesis and use of optically active Ru-complexes based on phosphonate  
19 functional groups compared to carboxylic counterparts.

## 20 21 22 23 Acknowledgement

24  
25 The Authors acknowledge the financial support from The Science and Technology Development  
26 Fund (STDF) provided by the Egyptian Government (Grant # 5415) and the IRD provided by the  
27 French Government (Grant # 005-2013)

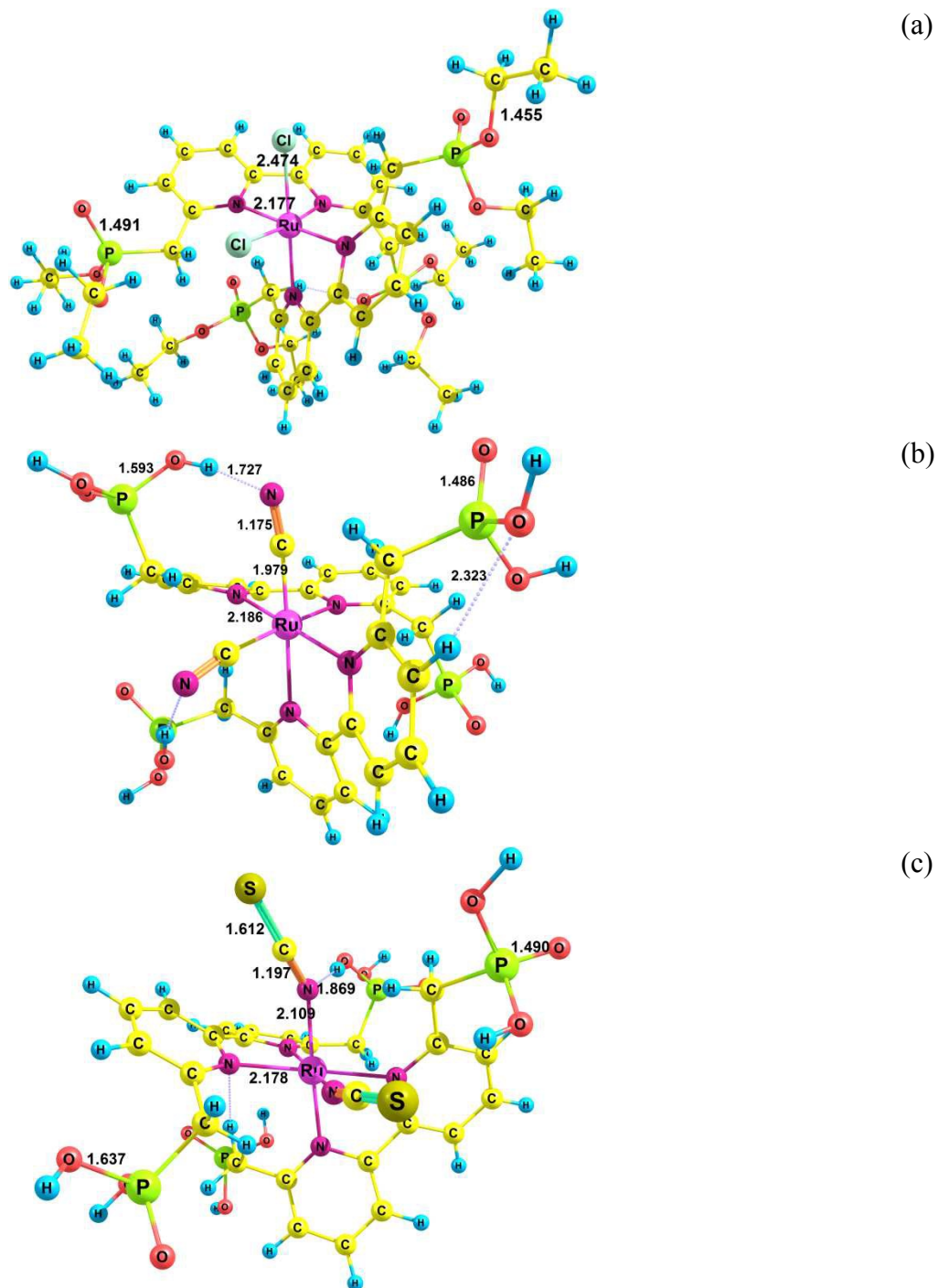
## 1 Reference

- 2
- 3 1. O'Regan, B.; Gratzel, M. *Nature* 1991, 353, 737-739.
- 4 2. Nazeeruddin, M. K.; Kay, A.; Rodicio, I.; Humphry-Baker, R.; Müller, E.; Liska, P.;
- 5 Vlachopoulos, N.; Grätzel, M. *J. Am. Chem. Soc.* 1993, 115, 6382-6390.
- 6 3. Argazzi, R.; Bignozzi, C. A.; Heimer, T. A.; Castellano, F. N.; Meyer, G. J. *Inorg. Chem.*
- 7 1994, 33, 5741-5749.
- 8 4. Ghosh, P.; Spiro, T. G. *J. Am. Chem. Soc.* 1980, 102, 5543-5549.
- 9 5. Bookbinder, D. C.; Wrighton, M. S. *J. Electrochem Soc.* 1983, 130, 1080-1086.
- 10 6. Miller, C. J.; Widrig, C. A.; Charych, D. H.; Majda, M. J. *J. Phys. Chem.* 1988, 92,
- 11 1928-1933.
- 12 7. T. H. Dunning Jr. and P. J. Hay, in *Modern Theoretical Chemistry*, Ed. H. F. Schaefer III,
- 13 Vol. 3 (Plenum, New York, 1976) 1-28.
- 14 8. W. R. Wadt and P. J. Hay, "Ab initio effective core potentials for molecular calculations -
- 15 potentials for main group elements Na to Bi," *J. Chem. Phys.*, 82 (1985) 284-98.
- 16 9. P. J. Hay and W. R. Wadt, "Ab initio effective core potentials for molecular calculations -
- 17 potentials for the transition-metal atoms Sc to Hg," *J. Chem. Phys.*, 82 (1985) 270-83.
- 18 10. P. J. Hay and W. R. Wadt, "Ab initio effective core potentials for molecular calculations -
- 19 potentials for K to Au including the outermost core orbitals," *J. Chem. Phys.*, 82 (1985)
- 20 299-310.
- 21 11. A. D. Becke *J. Chem. Phys.* 98 (1993) 5648.
- 22 12. C. Lee, W. Yang, R. G. Parr, *Phys. Rev. B* 37 (1988) 785.
- 23 13. B. Miehlich, A. Savin, H. Stoll, H. Preuss, *Chem. Phys. Lett.* 157 (1989) 200.
- 24 14. A.D. Becke, *J. Chem. Phys.* 98 (1993) 5648.
- 25 15. J.M. Martin, J. El-Yazal, J. Francois, *Mol. Phys.* 86 (1995) 1437.
- 26 16. Gaussian 09, Revision A.02, M. J. Frisch, G. W. Trucks, H. B. Schlegel, G. E. Scuseria, M.
- 27 A. Robb, J. R. Cheeseman, G. Scalmani, V. Barone, B. Mennucci, G. A. Petersson, H.
- 28 Nakatsuji, M. Caricato, X. Li, H. P. Hratchian, A. F. Izmaylov, J. Bloino, G. Zheng, J. L.
- 29 Sonnenberg, M. Hada, M. Ehara, K. Toyota, R. Fukuda, J. Hasegawa, M. Ishida, T.
- 30 Nakajima, Y. Honda, O. Kitao, H. Nakai, T. Vreven, J. A. Montgomery, Jr., J. E. Peralta, F.
- 31 Ogliaro, M. Bearpark, J. J. Heyd, E. Brothers, K. N. Kudin, V. N. Staroverov, R.
- 32 Kobayashi, J. Normand, K. Raghavachari, A. Rendell, J. C. Burant, S. S. Iyengar, J.
- 33 Tomasi, M. Cossi, N. Rega, J. M. Millam, M. Klene, J. E. Knox, J. B. Cross, V. Bakken,
- 34 C. Adamo, J. Jaramillo, R. Gomperts, R. E. Stratmann, O. Yazyev, A. J. Austin, R. Cammi,
- 35 C. Pomelli, J. W. Ochterski, R. L. Martin, K. Morokuma, V. G. Zakrzewski, G. A. Voth, P.
- 36 Salvador, J. J. Dannenberg, S. Dapprich, A. D. Daniels, O. Farkas, J. B. Foresman, J. V.
- 37 Ortiz, J. Cioslowski, and D. J. Fox, Gaussian, Inc., Wallingford CT, 2009.
- 38 17. <http://www.chemcraftprog.com>
- 39 18. GaussView, Version 5, Roy Dennington, Todd Keith, and John Millam, Semichem Inc.,
- 40 Shawnee Mission, KS, 2009.
- 41 19. S.G. Chen, S. Chappel, Y. Diamant, A. Zaban, *Chem. Mater.* 13 (2001) 4629.
- 42 20. S. Sakaki, T. Kuroki, T. Hamada, *J. Chem. Soc., Dalton Trans.* (2002) 840.
- 43 21. W. Sharmoukh and N. K. Allam. *Applied Materials and Interfaces*, 2012, 4 (8), pp 4413–
- 44 4418.
- 45 22. Elisabeth, Holder. Gabriele, Schoetz, Volker, Schurig and Ekkehard, Lindner.
- 46 *Tetrahedron; Asymmetry* 12(2001)2289-2293
- 47 23. George R. Newkome, Wallace E. Puckett, Garry E. Kiefer, Vinod K. Yuanjiao, Mark
- 48 Coreil, and Melisa A. Hackney. *J. Org. Chem.* 1982, 47, 4116- 4120.
- 49 24. Nazeeruddin, M. K.; Liska, P.; Vlachopoulos, N.; Gratzel, M. *J. Am. Chem. Soc.* 1993,
- 50 115, 6382-6390.
- 51 25. Argazzi, R.; Bignozzi, C. A.; Heimer, T. A.; Castellano, F. N.; Meyer, G. J. *Inorg.*
- 52 *Chem.* 1994, 33, 5741-5749.

- 1 26. Gratzel, M.; Kohle, O.; Nazeeruddin, M. K.; Pechy, P.; Rotzinger, F. P.; Ruile, S.;  
2 Zakeeruddin, S. M. In *PCT Int. Appl.*; Ecole Polytechnique Federale de Lausanne,  
3 Switz.: WO 95 29, 924, Nov. 1995; 52 pp.  
4 27. Katja Neuthe, Florian Bittner, Frank Stiemke, Benjamin Ziem, Juan Du, Monika Zellner,  
5 Michael Wark, Thomas Schubert, Rainer Haag; *Dyes and Pigments* 104 (2014) 24-33.  
6  
7  
8  
9  
10  
11  
12  
13  
14  
15  
16  
17  
18  
19  
20  
21  
22  
23  
24  
25  
26  
27  
28  
29  
30  
31  
32  
33  
34  
35  
36  
37  
38  
39  
40  
41  
42  
43  
44  
45  
46  
47  
48  
49

1 **Figures**

2



3

4 Figure 1. The optimized geometry of cis-Ru Complexes, bond lengths are shown in angstrom.

5

6

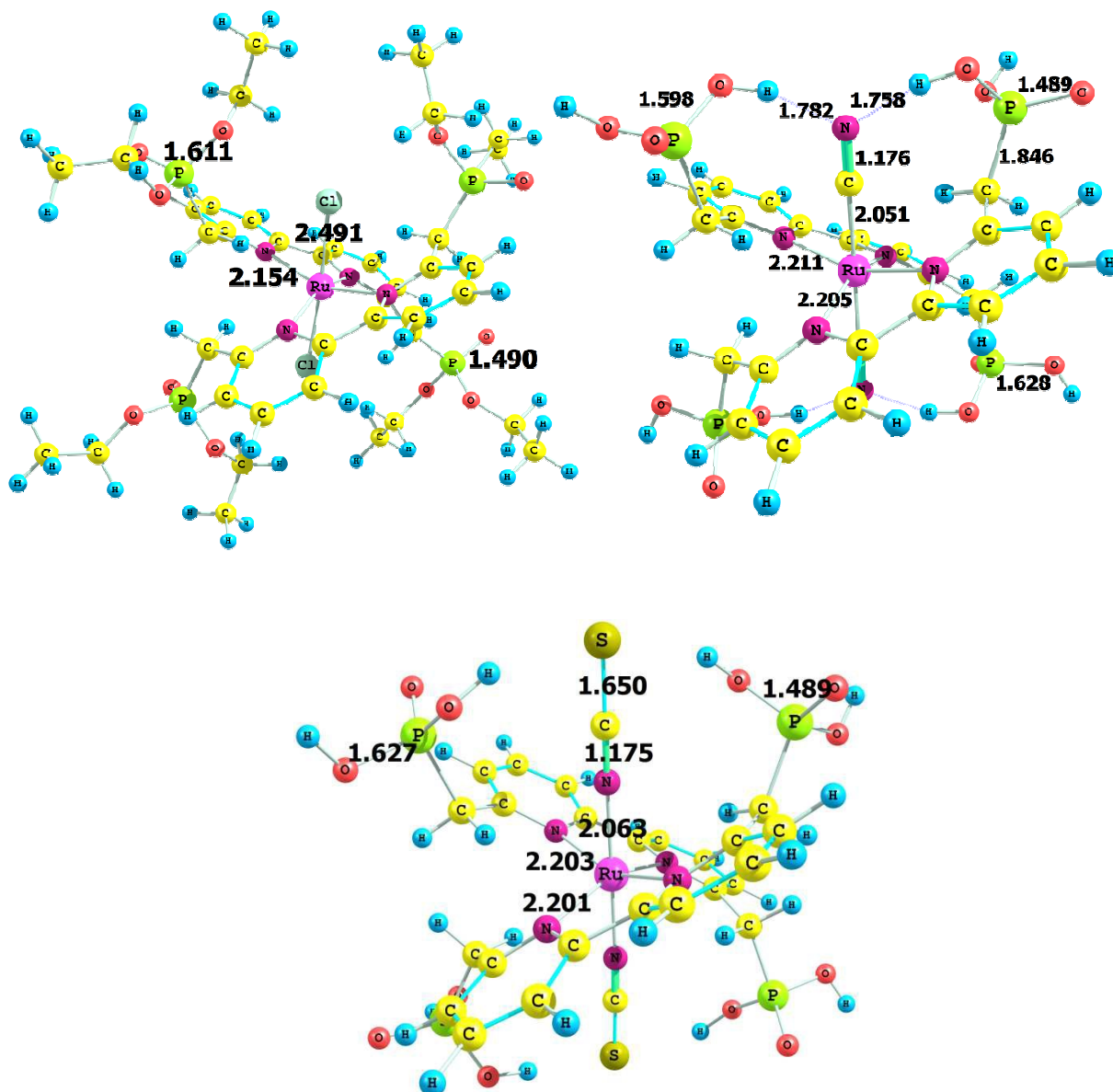


Figure 2. The optimized geometry of trans-Ru Complexes, bond lengths are shown in angstrom.

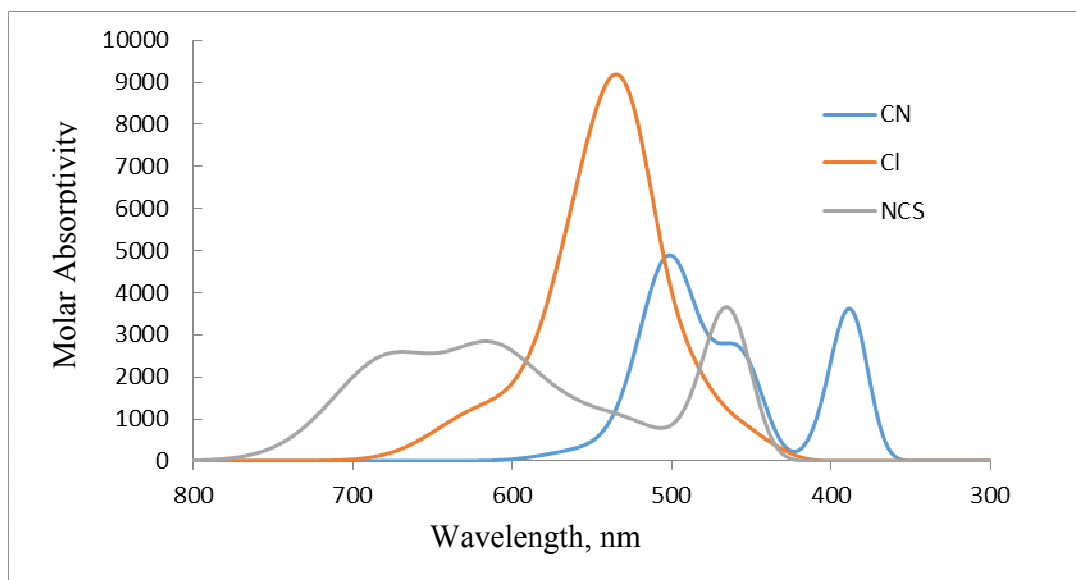


Figure 3. The theoretical electronic absorption spectra of the studied complexes

1  
2  
3  
4  
5  
6  
7  
8  
9  
10  
11  
12  
13  
14  
15  
16  
17  
18  
19  
20  
21  
22  
23  
24  
25  
26  
27  
28  
29  
30  
31  
32

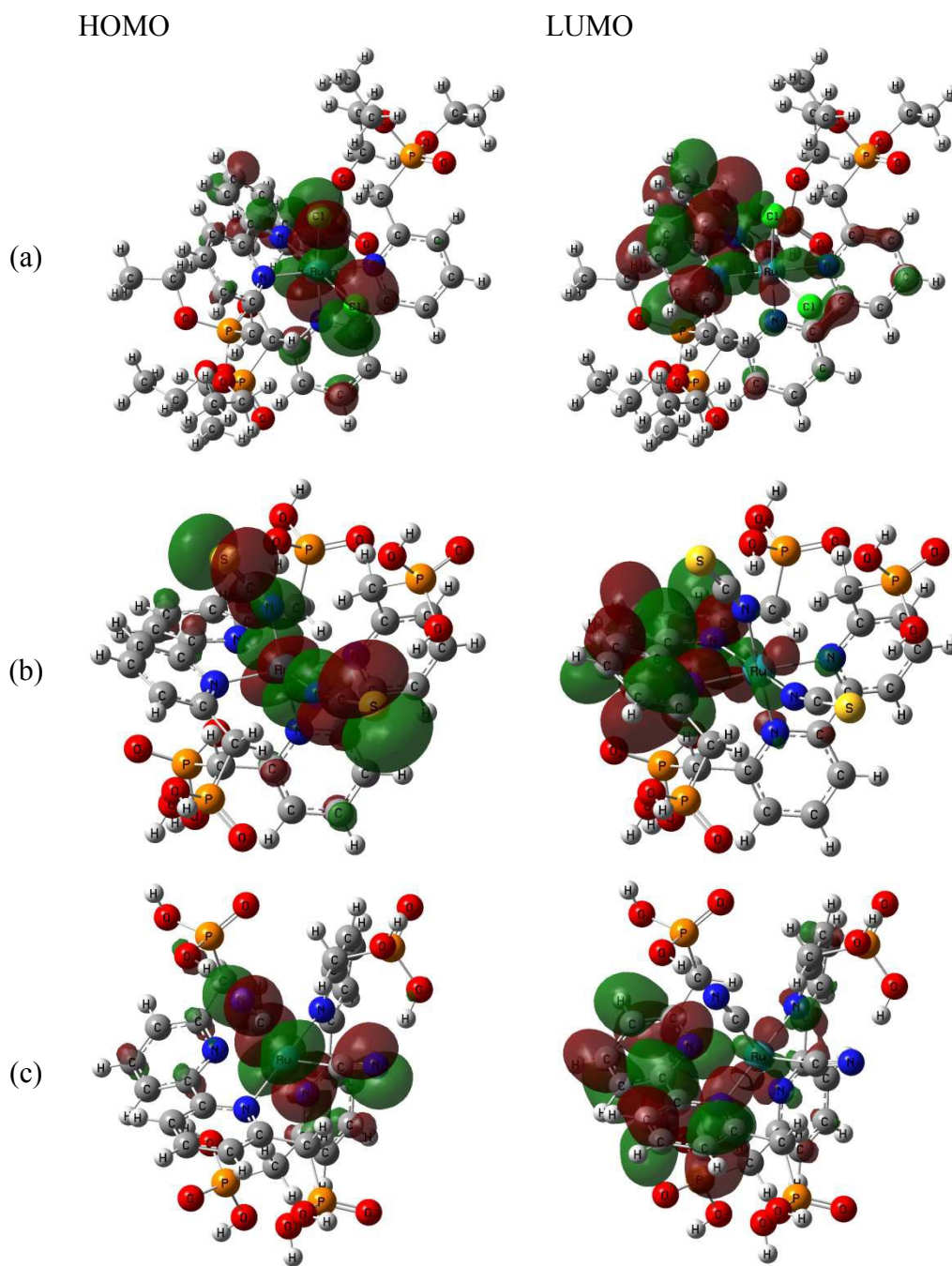
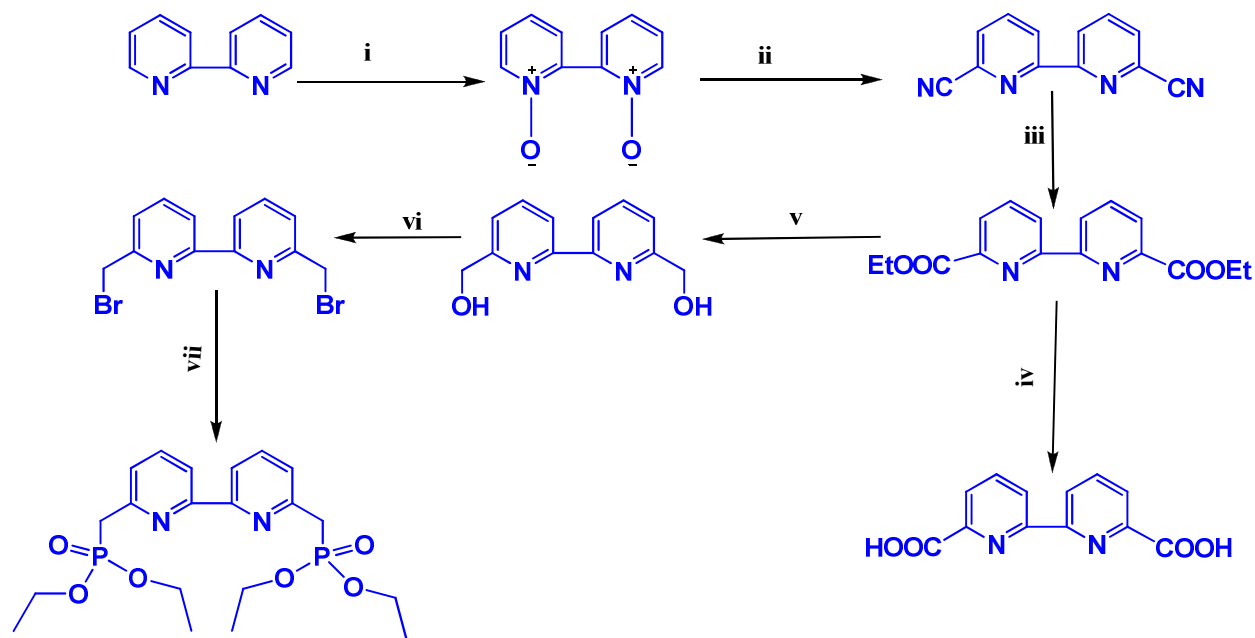


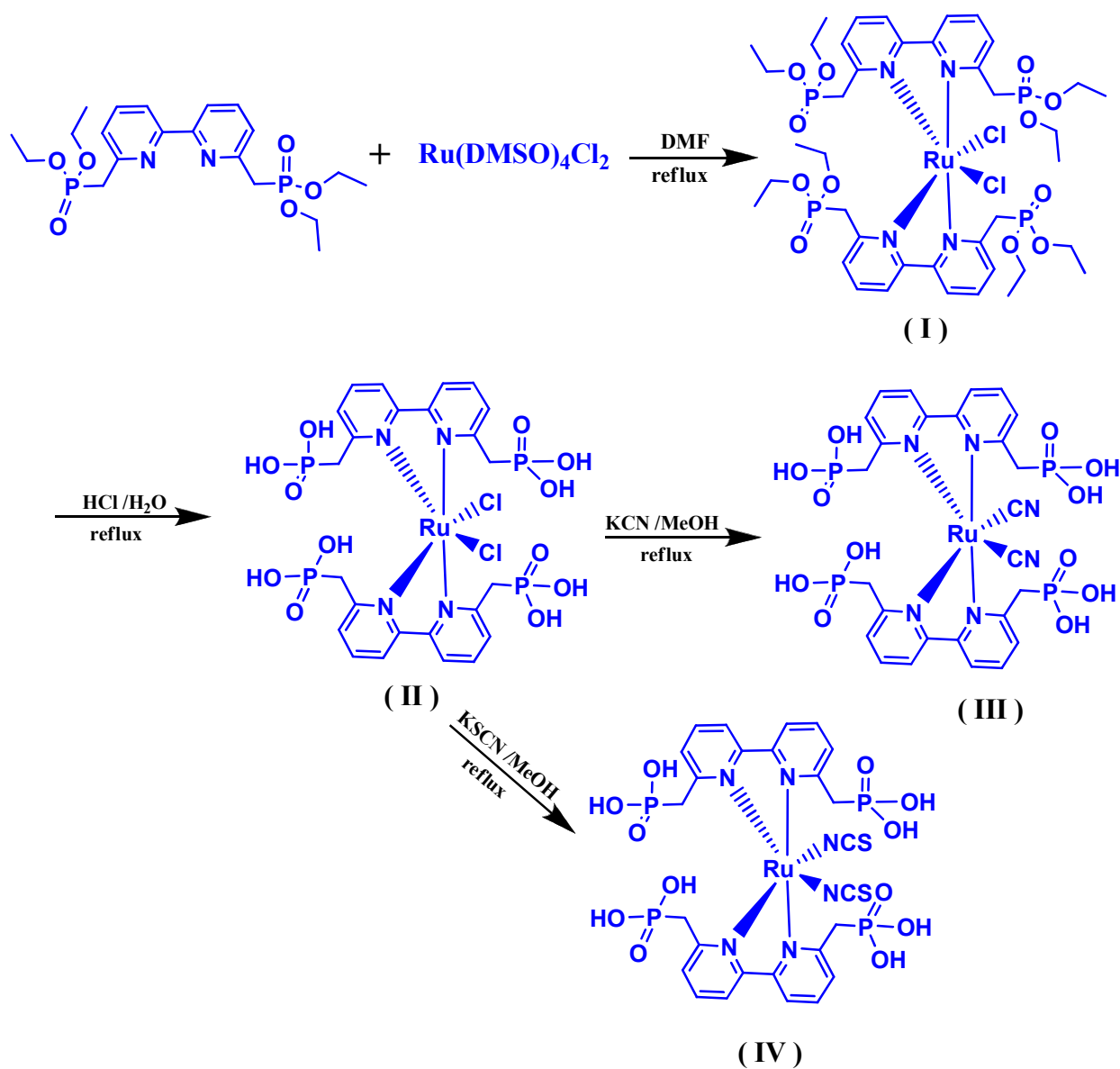
Figure 4. The HOMO and LUMO plots for (a) Cl, (b) NCS and (c) CN complexes

1  
2  
3  
4  
5  
6  
7



Scheme 1: Reaction and conditions: i) P-CPBA, CHCl<sub>3</sub> at 0 °C 2 d ii) KCN, H<sub>2</sub>O, PhCOCl, DCM, 12 h iii) EtOH, H<sub>2</sub>SO<sub>4</sub>, reflux, 12 h iv) NaOH, EtOH, Reflux 12 h v) NaBH<sub>4</sub>, DCM, r.t 6 h vi) HBr, H<sub>2</sub>SO<sub>4</sub>, reflux, 8 h vii) P(OEt)<sub>2</sub>, CHCl<sub>3</sub>, reflux 5 h.

1  
2  
3  
4  
5  
6  
7  
8  
9  
10



Scheme 2: Stepwise synthesis of the Ru-based complexes

1  
2  
3  
4  
5  
6  
7  
8  
9  
10  
11  
12  
13  
14  
15

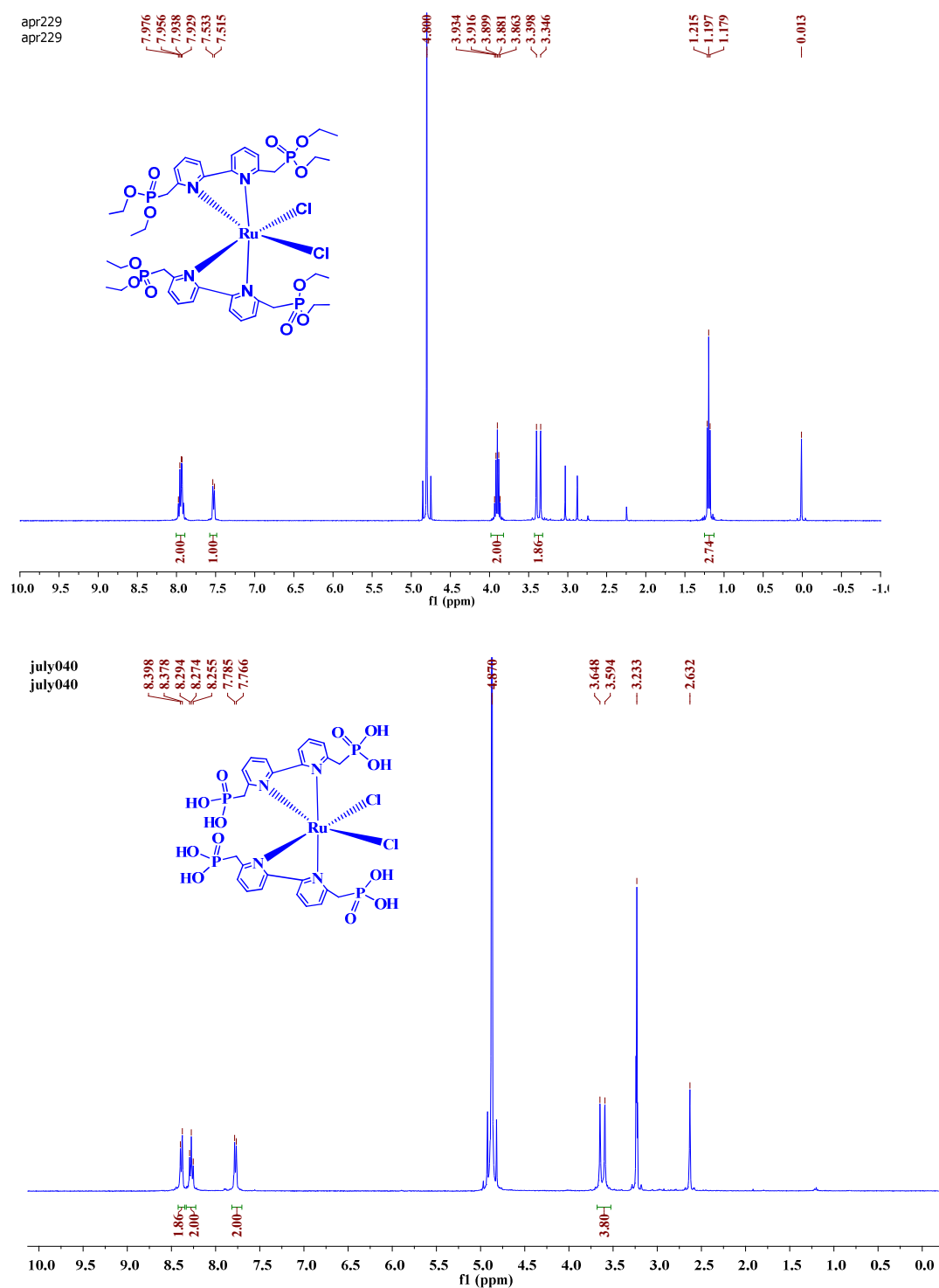


Figure 5.  $^1\text{H}$ NMR spectra of complex I and II recorded in  $\text{D}_2\text{O}$  and  $\text{CD}_3\text{OD}$

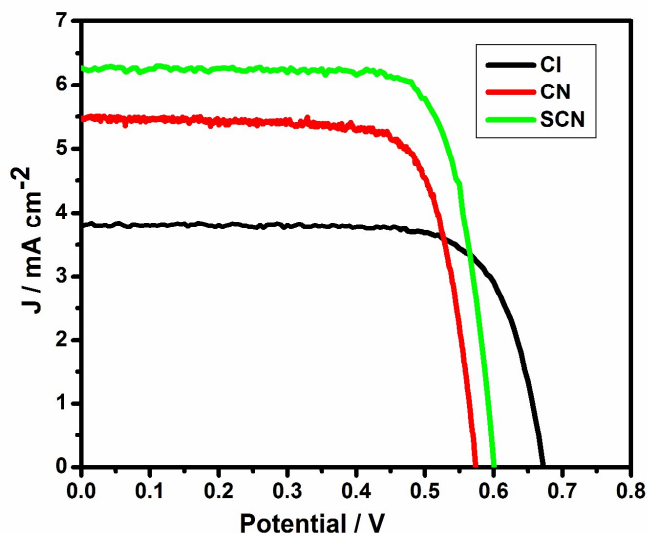


Figure 6.  $J-V$  characteristics of the solar cell devices measured under the irradiance of AM 1.5G full sunlight ( $100 \text{ mW cm}^{-2}$ ) with a cell active area of  $0.4 \text{ cm}^2$

## Tables

Table 1: The total energy  $E_T$ , difference in total energy  $\Delta E_T$  in Hartree,  $E_{\text{LUMO}}$ ,  $E_{\text{HOMO}}$ ,  $\Delta E$  in eV and dipole moment  $\mu$  (Debye) for complexes.

Configuration Complex	Trans			Cis		
	Cl	NCS	CN	Cl	NCS	CN
$E_T$ (a.u.)	-5062.31702835	-4495.03286616	-3698.63057783	-5062.3544477	-4495.04200812	-3698.63603973
$\Delta E_T$ (kcal/mol)	23.4810	5.7367	3.4274	0.0	0.0	0.0
$E_{\text{LUMO}}$ , eV	-2.358	-2.951	-2.957	-2.207	-2.9219	-2.856
$E_{\text{HOMO}}$ , eV	-5.065	-5.834	-6.446	-4.983	-5.3938	-5.897
$\Delta E$ , eV	2.706	2.883	3.489	2.776	2.472	3.041
$\mu$ , D	4.39	4.02	3.59	12.89	16.30	15.93

1 Table 2: The Ionization potential IE, Electron Affinity EA, energy of the first excited singlet  
2 state  $S_1$ , its Oscillator strength and Exciton binding energy for cis-complexes  
3

Cis Complexes	Cl	NCS	CN
IP, eV	5.901	6.510	7.019
EA, eV	-1.126	-1.1792	-1.704
TD-DFT $S_1$	1.9864	1.8205	2.2186
$f$	0.0075	0.0171	0.0017
$E_{\text{exciton}}$	0.7896	0.6515	0.8224

4 Table 3: The TDDFT results for singlet excited states with the highest oscillator strength.  
5  
6

Compound	State No.	Main Configuration	Coefficient	$f$	$\lambda$ , nm
Cl	$S_1$	H $\rightarrow$ L	0.61083	0.0075	624.2
	$S_3$	H-1 $\rightarrow$ L	0.55092	0.0284	558.9
	$S_4$	H-2 $\rightarrow$ L	0.57511	0.0521	530.2
CN	$S_1$	H $\rightarrow$ L	0.68420	0.0017	558.8
	$S_4$	H-2 $\rightarrow$ L	0.57914	0.0219	499.9
	$S_6$	H-1 $\rightarrow$ L+1	0.60695	0.0142	454.6
	$S_8$	H $\rightarrow$ L+4	0.42140	0.0184	387.9
NCS	$S_1$	H $\rightarrow$ L	0.67866	0.0171	681.0
	$S_2$	H $\rightarrow$ L+1	0.63450	0.0161	618.3
	$S_8$	H $\rightarrow$ L+2	0.41559	0.0081	471.6
	$S_{10}$	H $\rightarrow$ L+2	0.41978	0.0131	461.5

7  
8  
9  
10 Table 4: Comparison between photovoltaic parameters of the DSSCs prepared using different  
11 complexes.  
12

Dye	$J_{sc}$ [ $\text{mA cm}^{-2}$ ]	$V_{oc}$ [V]	$FF$	$\eta$ [%]
Cl	3.78	0.67	0.75	1.91
CN	5.47	0.57	0.76	2.38
SCN	6.27	0.60	0.77	2.9

13

## Graphical Abstract

